LETTER TO THE EDITOR

A single defect approximation for localized states on random lattices

G Biroli and R Monasson

CNRS, Laboratoire de Physique Théorique de l'ENS, 24 rue Lhomond, 75231 Paris, Cedex 05, France

E-mail: `biroli@physique.ens.fr` and `monasson@physique.ens.fr`

Abstract. Geometrical disorder is present in many physical situations giving rise to eigenvalue problems. The simplest case of diffusion on a random lattice with fluctuating site connectivities is studied analytically and by exact numerical diagonalizations. Localization of eigenmodes is shown to be induced by geometrical defects, that is sites with abnormally low or large connectivities. We expose a 'single defect approximation' (SDA) scheme founded on this mechanism that provides an accurate quantitative description of both extended and localized regions of the spectrum. We then present a systematic diagrammatic expansion allowing to use SDA for finite-dimensional problems, e.g. to determine the localized harmonic modes of amorphous media.

Since Anderson's fundamental work [1], physical systems in the presence of disorder are well known for exhibiting localization effects [2]. While most attention has been paid so far to Hamiltonians with random potentials (e.g. stemming from impurities), there are situations in which disorder also originates from geometry.

Of particular interest among these are the harmonic vibrations of amorphous materials such as liquids, colloids, glasses, etc around random particle configurations. Recent experiments on sound propagation in granular media [3, 4] have stressed the possible presence of localization effects, highly correlated with the microscopic structure of the sample. The existing theoretical framework for calculating the density of harmonic modes in amorphous systems was developed in liquid theory. In this context, microscopic configurations are not frozen but instantaneous normal modes (INM) give access to short time dynamics [5]. Wu and Loring [6] and Wan and Stratt [7] have calculated good estimates of the density of INM for Lennard-Jones liquids, averaged over instantaneous particle configurations. However, localization–delocalization properties of the eigenvectors have not been considered.

Diffusion on random lattices is another problem where geometrical randomness plays a crucial role [8]. Long-time dynamics is deeply related to the small eigenvalues of the Laplacian on the lattice and therefore to its spectral dimension. Campbell suggested that diffusion on a random lattice could also mimic the dynamics taking place in a complicated phase space, e.g. for glassy systems [9]. From this point of view, sites on the lattice represent microscopic configurations and edges represent allowed moves from one configuration to another. At low temperatures, most edges correspond to very improbable jumps and may be erased. The tail of the density of states of the Laplacian on random graphs was studied by means of heuristic arguments by Bray and Rodgers [10]. Localized eigenvectors, closely related to metastable states are of particular relevance for asymptotic dynamics.

Remarkably, the above examples lead to the study of the spectral properties of random symmetric matrices W sharing common features. In amorphous media, the elastic energy is a quadratic function of the displacements of the particles from their instantaneous 'frozen' positions. The INM are the eigenmodes of the stiffness matrix W. As for diffusion on random lattices, W simply equals the Laplacian operator. In both cases, each row of W is comprised of a small (with respect to the size N of the matrix) and random number of non-zero coefficients W_{ij} and most importantly, diagonal elements fluctuate: $W_{ii} = -\sum_{j(\neq i)} W_{ij}$†.

In this letter, we present a quantitative approach to explain the spectral properties and, particularly, localization effects of such a random matrix W in the simplest case, that is when all off-diagonal elements of W are independent random variables. Our analytical approximation is corroborated by exact numerical diagonalizations. We then expose a systematic diagrammatic expansion allowing for the study of more realistic models in the presence of correlated W_{ij}.

The spectral properties of W can be obtained through the knowledge of the resolvent $G(\lambda + i\epsilon)$: that is, the trace of $((\lambda + i\epsilon)\mathbf{1} - W)^{-1}$ [2]. Denoting the average over disorder by $\overline{(\cdot)}$, the mean density of states is given by

$$p(\lambda) = -\frac{1}{\pi} \lim_{\epsilon \to 0^+} \mathrm{Im}\, \overline{G(\lambda + i\epsilon)}. \tag{1}$$

The averaged resolvent is then written as the propagator of a replicated Gaussian field theory [2]:

$$\overline{G(\lambda + i\epsilon)} = \lim_{n \to 0} \frac{-i}{Nn} \int \prod_i \mathrm{d}\vec{\phi}_i \sum_{k=1}^{N} \vec{\phi}_k^2 \prod_i z_i \overline{\prod_{i<j}(1 + u_{ij})}$$

where

$$z_i \equiv z(\vec{\phi}_i) = \exp\left(\frac{i}{2}(\lambda + i\epsilon)\vec{\phi}_i^2\right) \tag{2}$$

$$u_{ij} = \exp\left(\frac{i}{2} W_{ij}(\vec{\phi}_i - \vec{\phi}_j)^2\right) - 1. \tag{3}$$

Replicated fields $\vec{\phi}_i$ are n-dimensional vector fields attached to each site i. To lighten notations, we have restricted ourselves in (3) to the scalar case. We shall focus later on W having an internal dimension, as in the INM problem.

In the uncorrelated case, the W_{ij} ($i < j$) are independently drawn from a probability law $\mathcal{P}$. To take into account geometrical randomness only, we focus on the distribution $\mathcal{P}(W_{ij}) = (1 - \frac{q}{N})\delta(W_{ij}) + \frac{q}{N}\delta(W_{ij} - w)$‡. Such a bimodal law merely defines a random graph: i and j can be said to be connected if and only if W_{ij} does not vanish. Due to the scaling of the edge-probability $\frac{q}{N}$, the mean site-connectivity q remains finite for large sizes N. We rescale the eigenvalues by choosing $w = -\frac{1}{q}$ to ensure that the support of the spectrum is positive and bounded when $q \to \infty$ [10].

Numerical diagonalizations of the random Laplacian W have been carried out for different sizes, up to $N = 3200$. To each eigenvector $\psi_{i,\ell}$ of eigenvalue λ_ℓ normalized to unity is associated the inverse participation ratio $w_\ell^4 = \sum_i |\psi_{i,\ell}|^4$. We then define $w^4(\lambda)\,\mathrm{d}\lambda$ as the

---

† Such W matrices are indeed expected in systems where $(1, 1, \ldots, 1)$ is an eigenvector with zero eigenvalue: the elastic energy is left unchanged under a global translation of all particles whereas, in the diffusion case, the equilibrium probability distribution is uniform over all sites.

‡ For simplicity we have not considered fluctuations of the connections strengths. To take into account the latter, one has only to average the last term of equation (4) over the probability law of w. For a Cauchy distribution we have verified that EMA is already able to capture localization effects due to fluctuations of w; whereas SDA accounts also for local geometric fluctuations and is in better agreement with numerical results. Notice that the fluctuations of w smear out the peaks observed in figure 1.
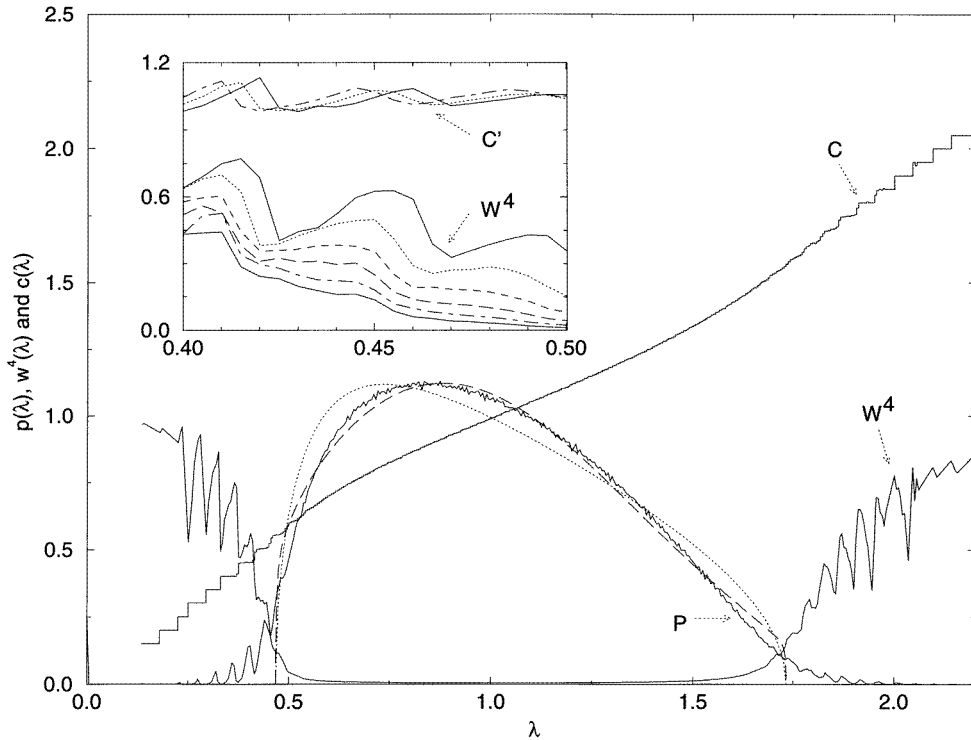
Figure 1. Density of states $p(\lambda)$, inverse participation ratio $w^4(\lambda)$ and connectivity of the centres $c(\lambda)$ (divided by q) averaged over 2000 samples for $q = 20$, $N = 800$ (all solid curves). The bottom parts of the oscillations of w^4 at small and large λ are suppressed due to the statistical shortfall of eigenvalues. Dotted and dashed curves respectively show the EMA and (the extended region of) the SDA spectra. Inset: oscillations of $w^4(\lambda)$ for $N = 100, 200, 400, 800, 1600$ and 3200 from top to botton and fluctuations of $c'(\lambda)$ (divided by q) for $N = 100, 200, 1600$ (same symbols) and $0.4 \leqslant \lambda \leqslant 0.5$.

sum of w_ℓ^4 over all $\psi_{i,\ell}$ lying in the range $\lambda \leqslant \lambda_\ell \leqslant \lambda + d\lambda$, divided by the number $Np(\lambda)\, d\lambda$ of such eigenvectors. Figure 1 displays $p(\lambda)$ and $w^4(\lambda)$ for a mean connectivity $q = 20$†. The central part of the spectrum ($\lambda_- < \lambda < \lambda_+$) has a smooth bell shape and corresponds to extended states. For increasing sizes N and at fixed λ, w^4 vanishes as $1/N$ and the breakdown of this scaling identifies the mobility edges: $\lambda_- \simeq 0.47 \pm 0.01$ and $\lambda_+ \simeq 1.67 \pm 0.03$. Outside the central region, that is for small or large eigenvalues, the eigenstates become localized and the density exhibits successive regular peaks.

We have measured for each eigenvector $\psi_{i,\ell}$ the connectivity c_ℓ of its centre, that is the site i_0 with maximum component $|\psi_{i_0,\ell}|$. The mean connectivity $c(\lambda)$ of the centres of eigenvectors having eigenvalue λ is plotted figure 1. It is a smooth monotonous function of λ in the extended part of the spectrum. In the localized region, $c(\lambda)$ is constant over a given peak and integer-valued ($c \leqslant c_- = 10$ on the left side of the spectrum, $c \geqslant c_+ = 33$ on the right side); the centre connectivity abruptly jumps when λ crosses the borders between peaks. Furthermore, table 1 shows the good agreement between the weight of peak associated to connectivity c and the fraction of sites having c neighbours, given by a Poisson law of parameter q†.

Therefore, numerics indicate that localized eigenvectors are centred on geometrical

† We have chosen $q \gg 1$ to avoid trivial localization effects due to non-percolating isolated clusters of sites. Similar

Table 1. Weights p (i.e. integrated density of eigenvalues belonging) of the peaks and corresponding eigenvalues λ obtained from numerical simulations (NUM) and SDA for low connectivities c. λ^{NUM} is measured at the top of the peak with absolute error ± 0.0025 whereas the relative error on p^{NUM} is about 10% (except for the $c = 10$ peak). A similar agreement is reached for large connectivities.

c	3	4	5	6	7	8	9	10
λ^{NUM}	0.138	0.185	0.230	0.275	0.320	0.360	0.402	0.440
λ^{SDA}	0.140	0.186	0.231	0.276	0.319	0.361	0.400	0.435
$p^{NUM} \times 10^4$	0.025	0.096	0.566	1.607	4.70	10.75	25.14	<50
$p^{SDA} \times 10^4$	0.027	0.134	0.532	1.747	4.88	11.76	24.54	42.85

defects, that is on sites whose number of neighbours is much smaller or much larger than the average connectivity. To support this observation, it is instructive to consider a simpler model including a unique defect, i.e. a Cayley tree with connectivity c for the central site and $q + 1$ for all other points [11] (locally a random graph is equivalent to a tree since no loops of finite length are present). Looking for a localized state ψ_i with a radial symmetry $\psi_i = \psi_{d(i)}$ where $d(i)$ is the distance between site i and centre, the eigenvalue equations read $c(\psi_0 - \psi_1) = q\lambda\psi_0$ and $(q + 1)\psi_d - q\psi_{d+1} - \psi_{d-1} = q\lambda\psi_d$ for $d \geqslant 1$ [11]. The eigenvalue problem reduces to the search of the solution of a homogeneous linear difference equation of order two (equation for $d \geqslant 1$) fulfilling a boundary condition (equation for $d = 0$). After a little algebra we have found that strong defects, such that $|q - c| > \sqrt{q}$ give rise to localized states around the central site with an eigenvalue $\lambda = \frac{c}{q}(1 - \frac{1}{q-c})$. The predicted connectivities at mobility edges ($c_- = 15$ and $c_+ = 25$ for $q = 20$) are in poor agreement with numerical findings. A more refined picture requires one to take into account the connectivity fluctuations of the neighbours of the central site. We have thus considered a Cayley tree with a coordination number c for the central site, c' for the nearest neighbours and $q + 1$ for all other points. We have found that localized states due to weak (resp. strong) central connectivity c can disappear and become extended if the connectivity of the neighbours c' reaches large (resp. small) values. In other words, a defect can be *screened* by an opposite connectivity fluctuation of its surrounding neighbours. Numerics supports this scenario. As λ varies, $w^4(\lambda)$ exhibit oscillations (interpreted as finite-size contributions coming from extended states) of rapidly decreasing amplitudes with increasing N. These oscillations are correlated (positively for small c and negatively for large c) with the fluctuations of the neighbours connectivity $c'(\lambda)$ around its mean value $q + 1$, see inset of figure 1.

Let us see how the above results may be recovered from theory. Due to the statistical independence of the W_{ij}, the u_{ij} (3) interactions are averaged out separately [10]. The resulting theory is, of course, invariant under any relabelling of the sites i and depends on the fields $\vec{\phi}_i$ through the density $\rho(\vec{\phi})$ of sites i carrying fields $\vec{\phi}_i = \vec{\phi}$ only [12]. The functional order parameter $\rho(\vec{\phi})$ is found when optimizing the 'free-energy' [10, 12]

$$\ln \Xi[\rho] = \int d\vec{\phi}\, \rho(\vec{\phi})[\ln z(\vec{\phi}) - \ln \rho(\vec{\phi}) + 1] + \frac{q}{2} \int d\vec{\phi}\, d\vec{\psi}\, (e^{-i(\vec{\phi}-\vec{\psi})^2/2q} - 1)\rho(\vec{\phi})\rho(\vec{\psi}) \quad (4)$$

under the normalization constraint $\int d\vec{\phi}\, \rho(\vec{\phi}) = 1$; $z(\vec{\phi})$ has been defined in (2). This order

results have been obtained for $q = 10$.
† Simulations on random lattices with *fixed* connectivity $q = 20$ show no localization eigenstates. The resulting spectrum is in excellent agreement with the EMA prediction.

parameter is simply related to the original random matrix problem through

$$\rho(\vec{\phi}) = \frac{1}{N} \overline{\sum_{i=1}^{N} C_i \exp\left(\frac{i\vec{\phi}^2}{2[(\lambda + i\epsilon)\mathbf{1} - W]_{ii}^{-1}}\right)}. \tag{5}$$

The C_i are normalization constants going to unity as n vanishes. Therefore, the averaged resolvent reads $\overline{G(\lambda + i\epsilon)} = -i \lim_{n \to 0} \int d\vec{\phi} \, \rho(\vec{\phi})(\phi^1)^2$.

Finding an exact solution to the maximization equation $\delta \ln \Xi / \delta \rho(\vec{\phi}) = 0$ seems to be a hopeless task. This is a general situation, which arises in the study of the physics of dilute systems (for the case of sparse random matrices see, for example, [10, 13]). Identity (5) may, however, be used as a starting point for an effective medium approximation (EMA). In the extended part of the spectrum, we expect all matrix elements appearing in (5) to be of the same order of magnitude and thus $\rho(\vec{\phi})$ to be roughly Gaussian. EMA is therefore implemented by inserting the Gaussian ansatz

$$\rho^{EMA}(\vec{\phi}) = (2\pi i g(\lambda))^{-\frac{n}{2}} \exp\left(\frac{i\vec{\phi}^2}{2g(\lambda)}\right) \tag{6}$$

into functional Ξ (4). The average EMA resolvent g is then obtained through optimization of $\ln \Xi[g(\lambda)]$. The resulting spectrum, which is given by the imaginary part of g divided by minus π, is shown in figure 1. As expected, EMA gives a sensible estimate of the spectral properties in the extended region and of the mobility edges $\lambda_-^{EMA} = 0.468$, $\lambda_+^{EMA} = 1.732$. However, EMA is intrinsically unable to reflect geometry fluctuations and thus the presence of localized states (see footnote, p 258).

To do so, we start by writing the extremization condition of $\ln \Xi$ over ρ as

$$\rho(\vec{\phi}) = \mathcal{H}[\rho](\vec{\phi}) \tag{7}$$

where the functional $\mathcal{H}$ may be expanded as

$$\mathcal{H}[\rho](\vec{\phi}) = hz(\vec{\phi}) \sum_{k=0}^{\infty} \frac{e^{-q} q^k}{k!} \left[\int d\vec{\psi} \, \rho(\vec{\psi}) e^{-i(\vec{\phi} - \vec{\psi})^2/2q}\right]^k. \tag{8}$$

h is a multiplicative factor equal to unity in the $n \to 0$ limit. Equations (7) and (8) describe an elementary lattice of one central site connected to k neighbours according to a Poisson distribution of mean q. Neighbours carry information about the random matrix elements through the order parameter $\rho(\vec{\psi})$ (5) and interact with the central site via kernel $\exp(-i(\vec{\phi} - \vec{\psi})^2/2q)$ ((3), (8)). Self-consistency requires that the resulting order parameter at central site equals ρ [14]. Bearing in mind the localization mechanism unveiled in previous paragraphs, we propose a *single defect approximation* (SDA). SDA amounts to making the central site interact with k neighbours belonging to the effective medium defined above. Since EMA precisely washes out any local geometrical fluctuation, we partially reintroduce them by allowing the connectivity k of the central site (the defect) to vary. The SDA order parameter is thus obtained through an iteration of equation (7)

$$\rho^{SDA}(\vec{\phi}) = \mathcal{H}[\rho^{EMA}](\vec{\phi}). \tag{9}$$

Using the EMA resolvent g (6), we have computed the SDA spectrum for $q = 20$. The SDA extended part is shown to be in better agreement with numerical results than the EMA in figure 1. Improvement is even more spectacular for localized states that were absent within EMA. We have found Dirac peaks whose weights and eigenvalues are listed table 1. The agreement with numerical results is quite good. We have verified analytically that SDA peaks do correspond to localized states by calculating $\lim_{\epsilon \to 0} [\epsilon \overline{G(\lambda + i\epsilon) G(\lambda - i\epsilon)}]$ [15] using SDA

with two groups of replicas. This quantity gives also access to $w^4(\lambda)$, whose value seems slightly higher than numerical measures close to the mobility edges.

Starting from any sensible ρ, successive iterations of equation (7) would also provide more and more accurate descriptions of the 'fractal' structure of the localized peaks but at the price of heavier and heavier calculations. Besides being theoretically founded, SDA has the advantage that a single iteration from EMA (which is easily computable) succeeds in capturing localized states in a quantitative way (see footnote, p 256).

In general, the components of W are correlated and the average over disorder requires an expansion in terms of the connected correlation functions of the u_{ij} interactions

$$\overline{\prod_{i<j}(1+u_{ij})} = \exp\left(\sum_{i<j}\overline{u_{ij}} + \tfrac{1}{2}\sum_{i<j,k<l}' \overline{u_{ij}u_{kl}}^c + \cdots\right) \tag{10}$$

where the prime indicates that the sum runs over different pairs of sites. Free energy (4) corresponds to the case where all terms in (10) but the first one vanish. The presence of these cumulants (of order 2, 3, ... in u) will result in the addition of cubic, quartic, etc $\rho(\vec{\phi})$ interactions terms to $\ln \Xi$. Although calculations become more difficult, the existence of a variational free energy $\ln \Xi$ is preserved. This is all that is needed to derive EMA and the optimization equation (9).

Let us see how SDA can be implemented to determine the INM spectrum of amorphous media. We restrict ourselves to liquids but our approach could also be applied to glasses using the formalism recently developed by Mézard and Parisi [16]. Particles i are individuated by their positions x_i and interact through a two-body potential $V(x_i - x_j)$ (hereafter bold letters will denote vectors in the D-dimensional real space). For a given microscopic configuration, INM are the eigenmodes of the $D \times N$-dimensional matrix $W_{ij} = \partial^2 V(x_i - x_j)/\partial x_i \partial x_j$ $(i \neq j)$. The calculation of the spectrum and the average over particle configurations (with the equilibrium Boltzmann measure at inverse temperature β) can be performed at the same time by introducing a generalized liquid [6, 7]. Each particle is assigned a 'position' $r_i = (x_i, \vec{\phi}_i)$ and the generalized fugacity reads $z^*(r_i) = yz(\vec{\phi}_i)$ where y is the liquid fugacity and z is defined in (2). The grand-canonical partition function Ξ may then diagrammatically expanded in powers of the Mayer bond $b(r_i, r_j) = \exp(-\beta V(x_i - x_j) + \tfrac{1}{2}W_{ij}(\vec{\phi}_i - \vec{\phi}_j)^2) - 1$ (for the sake of simplicity, the summation over the D^2 internal indices of W is not written explicitly). With these notations, Ξ coincides with formula (3.21) of [17]. It is now straightforward to take advantage of the variational formulation of the diagrammatic virial expansion by Morita and Hiroike [17]. The generalized density $\rho(r) = \rho(x, \vec{\phi})$ of particles optimizes

$$\ln \Xi[\rho] = \int dr\, \rho(r)[\ln z^*(r) - \ln \rho(r) + 1] + \mathcal{S} \tag{11}$$

where $\mathcal{S}$ is the sum of all diagrams composed of bonds $b(r, r')$ and vertices weighted with $\rho(r)$ that cannot be split under the removal of a single vertex, see equation (4.6) of [17]. Due to translational invariance in real space, ρ does not depend on x and we are left with a variational functional Ξ of the density $\rho(\vec{\phi})$. Note that (11) contains (4) as a special case when $\mathcal{S}$ includes only the simplest single-bond diagram. The random graph model we have studied in this letter may be seen as a physical system for which keeping the first coefficient of the virial expansion only is exact.

To our knowledge, Morita and Hiroike's work has not been used so far in the context of INM theory as a short-cut to avoid tedious diagrammatical calculations. In addition, the variational formulation of [17] allows one to implement SDA in a practical way. We are currently attempting to apply the present formalism to characterize localized eigenstates in two- and three-dimensional granular media.

References

[1] Anderson P W 1958 *Phys. Rev.* **109** 1492
[2] Thouless D J 1974 *Phys. Rep.* **13** 93
    Thouless D J 1995 *Mesoscopic Quantum Physics (Les Houches Session LXI)* (Amsterdam: Elsevier)
[3] Liu C H and Nagel S R 1992 *Phys. Rev. Lett.* **68** 2301
[4] Jia X, Caroli C and Velicky B 1999 *Phys. Rev. Lett.* **82** 1863
[5] Keyes T 1997 *J. Phys. Chem.* A **101** 2921
[6] Wung T-M and Loring R 1992 *J. Chem. Phys.* **97** 8568
[7] Wan Y and Stratt R 1994 *J. Chem. Phys.* **100** 5123
[8] Havlin S and Ben Avraham D 1987 *Adv. Phys.* **36** 695
[9] Campbell I A 1985 *J. Physique Lett.* **46** L1159
[10] Bray A J and Rodgers G J 1988 *Phys. Rev.* B **38** 11 461
[11] Thouless D J 1998 Private communication
[12] Monasson R 1998 *J. Phys. A: Math. Gen.* **31** 513
[13] Rodgers G J and Bray A J 1988 *Phys. Rev.* B **37** 3557
     Rodgers G J and De Dominicis C 1990 *J. Phys. A: Math. Gen.* **23** 1567
     Mirlin A D and Fyodorov Y V 1991 *J. Phys. A: Math. Gen.* **24** 2273
[14] Abou-Chacra R, Anderson P W and Thouless D J 1973 *J. Phys. C: Solid State Phys.* **6** 1734
[15] Cohen M H and Economou E N 1971 *Phys. Rev.* B **5** 293
[16] Mézard M and Parisi G 1999 *Phys. Rev. Lett.* **82** 747
[17] Morita T and Hiroike K 1961 *Prog. Theor. Phys.* **25** 537